

## DWT Based Method to Locate Tumor from T2-W Axial Head Scans

S. Karthigai Selvi

Department of Computer Science and Applications, The Gandhigram Rural Institute – Deemed to be University, India, 624302.

**ABSTRACT** -This paper proposes a novel wavelet based feature set to analyze the T2 weighted axial images to classify tumour distress slices and locate tumour tissues by using Mean absolute percentage error (MAPE). The nature of brain is almost symmetry and having more number of components such as sulcus, gyrus, ventricles and CSF. These are all forming more edges in MRI image. Thus induces to define a strategic wavelet feature set to recognize tumour distress images. This paper delineates a novel feature set and its efficiency in classification. This feature sets employed in support vector machine (SVM) to classify the abnormal slices. Then exact tumour location was detected using MAPE. It is also compared against existing Gray level co-occurrence matrix (GLCM) based feature set and an unsupervised algorithm in terms of false alarm and missed alarm. The final tumour location detection compared against the Wavelet packet based method (Wpack ).

**Index Terms** - Wavelet, feature, MRI image, normal, abnormal, SVM, Wavelet packet transformation

Date of Submission: 30-03-2019

Date of acceptance: 13-04-2019

### I. INTRODUCTION

A brain tumour is a mass or growth of abnormal cells such as neoplasm in a brain or close to a brain. MRI is the most effective tool to diagnose a brain tumour. Its multi planner capability, superior contrast resolution and flexible protocols allows it to be a more vital tool in diagnosis process such as directing biopsies, in planning the proper therapy and in evaluating the therapeutic results. MRI machines can produce different tissue contrast images due to its varying excitation and repetition time. They are referred in terms of T1-weighted (T1-w), T2 weighted (T2-w) and T1 contrast (T1-c) images [1]. The radiological definition of the tumour margins in the clinical contrast are often manually determined by the radiologists on the T2-w images [2] because CSF, tumour and edema are in hyper intense. However, MRI machine produces hundreds of images per patient. Hence, an automatic tool emerges to reduce radiologist time by classifying abnormal slices. It motivates researchers to fabricate an automatic abnormal image classification technique.

Several similarity based methods were developed to do this work. Somasundaram and Kalaiselvi proposed a novel work which uses fuzzy measures [3]. In this work, image alignment was done by fitting a symmetric line between two hemispheres. Then by using fuzzy clustering algorithm extract lesion pixels and CSF. Finally, fuzzy symmetry measure concludes abnormal images. Another work employed fast unsupervised change detection method [4]. It is searching dissimilar regions across the symmetry line of the brain using the Bhattacharya

coefficient score. Kalaiselvi et al. proposed an algorithm which was developed using a novel statistical feature to detect abnormal images in T2- w images. It uses a novel weighted mean. It also discards the normal volumes [5]. These are all unsupervised algorithms.

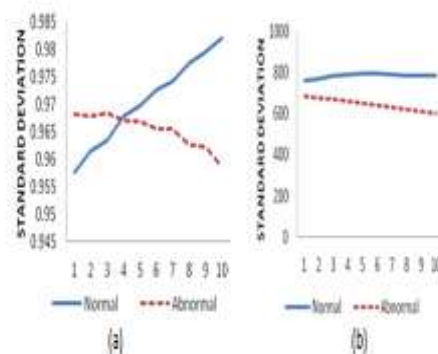


Figure 1. Standard deviation of normal and abnormal images from a volume. (a) standard deviation obtained from original image. (b) Standard deviation obtained from approximation section.

For supervised algorithm, support vector machine (SVM), k-nearest neighbor algorithms (KNN), neural networks (NN) and Genetic algorithms (GA) have been using for classification. It uses feature sets such as intensity based features, texture features and shape features. Features are representing images in an alternate way by measuring certain properties of the images. It can distinguish an image from other images [6]. More features are currently used in medical image analysis. The features which

are extracted directly from images are called first order features. The features which encompass neighbourhood pixels and transformation are called second order features. The second order features represents the texture of the image. They are also called as texture features. GLCM and wavelets are the best tools to extract second order features. Generally, texture feature extraction uses wavelet which is a mathematical function and by using its scaled and translated copies, analyzes an image into different frequency components at different scales [7]. Another texture feature extraction tool is gray level co-occurrence matrix (GLCM). It depends on intensity of neighbouring pixels.

The classifier SVM is a binary classification method to minimize structural risk. It is an attractive and systematic method for two class problems. It uses learning algorithms that would analyze data recognize patterns. It makes use of training datasets to build support vectors in training stage. With the support vectors it can able to classify unknown data sets. The researchers make use of classifiers with different feature sets to detect abnormal images.

More statistical and GLCM based feature sets were implemented in least square SVM (LSSVM) which uses least square measure instead of hyper plane in SVM [8]. While comparing the results of SVM with K-NN and LS-SVM, LS-SVM produces better results. One existing algorithm uses hybrid technique which uses SVM and fuzzy concept. It is referred in terms of Fuzzy support vector machine (FSVM). It uses GLCM based features for training and classification [9]. Along with the GLCM based features, Wavelet based features were employed to train the SVM classifier [10]. The wavelet features were extracted by applying discrete wavelet transformation (DWT) up to two levels. Then the statistical measures of all sub bands are taken for the classification. Some researchers analyze the SVM training algorithms (kernels) to make use of abnormal image classification. Satish et. al employed RBF kernel of SVM to classify abnormal images [11]. It outperforms Adaboost classifier. In some existing works, principal component analysis (PCA) reduces the feature set. The reduced features were given to SVM classifier [12]. Another work uses Gabor wavelets for feature extraction [13]. It has been used to train NN to classify abnormal images [14]. Then, it uses PCA to reduce features and then employs in Back propagation NN to classify abnormal images.

Tumour and CSF separation in T2-w images is hard in machine vision. An existing work Wpack locate tumour tissues using wavelet packet based feature set and modulus maxima [7]. The proposed work uses MAPE error measure. Usually, it is used to estimate the financial forecast error. But it is applied in this work to estimate the inhomogeneity of pixels in a block.

The above stated methods are using denoising process in its process pipeline. The classification algorithms are using more number of features, and then PCA is used to reduce the feature set. It consumes more time in classification work. To avoid these steps, this paper introduces a novel DWT based feature. DWT uses low and high pass filter banks that would separate low and high frequency image contents separately. Among them, the proposed method uses mainly low passed content. Hence, high frequency noises will be avoided in the proposed work.

The remaining paper is organized as follows, section 2 describes the method and discusses a novel wavelet feature which is helps for classification technique and tumour location detection, section 3 discusses the results of proposed method and section 4 concludes the results.

## II. METHOD

This method uses an existing method 2D-BEA to extract brain from its surrounding [15]. A novel DWT based feature set is extracted based on the knowledge of brain anatomy and characteristics of DWT. Then make use of the feature set, classification is done by using the SVM classifier. From the classified abnormal slices, the exact tumour location was detected using MAPE error measure. It consists of 4 stages. They are

- Stage 1: Brain extraction
- Stage 2: Wavelet feature extraction
- Stage 3: Classification
- Stage 4: Tumour location detection

### A. Brain Extraction

Somasundaram and Kalasiselvi proposed a brain extraction algorithm 2D-BEA for T2-w images [15]. This method uses diffusion concept to enhance the brain boundaries, then using Ridler's thresholding technique rough binary brain image is obtained. By employing morphological operations and using the largest connected component analysis, a brain mask is obtained to extract brain.

### B. Wavelet Based Feature Extraction

Brain images have more edge information due to sulci, gyri, CSF, Neoplasm and glial cells. It affects some first order features to distinguish normal and abnormal images. It is demonstrated in Fig.1. Fig.1 (a) shows the standard deviation of the normal and abnormal images. But it does not distinguish normal and abnormal images. Hence, we go for wavelet feature. Wavelets are local in both frequency and space. Especially, DWT provides a compact representation of signal frequency components with strong spatial support. It decomposes a signal into frequency sub bands at different scales. Another

advantage of DWT is that it avoids denoising techniques in low noise level because images are low passed contents and the edges and noises are high passed contents. DWT makes use of low passed content sub bands alone. The sub band which is processed by the low pass filters along row and column called as approximation section LL. It contains low pass contents which resembles images. It is also called approximation section a. The sub bands which are processed by the low and the high pass filters are called detail sections d.

The next level of resolution analysis is obtained by again decompose the LL. While removing the high frequency contents, the normal and abnormal images have distinct standard deviation in approximation section a. It is graphically represented in Fig 1(b).

A novel feature is obtained by decomposing the image  $IN \times N$  until to achieve  $110 \times 14$ . In this work the image size was reduced or increased by linear interpolation to normalize the image size as  $1216 \times 160$ . While considering LL at this level, the tumour region shows in higher intensity. Mostly, axial images have CSF in its centre. If tumour distress in any location of the hemispheres, that will contain maximum value, it helps to identify the abnormal images. For better interpretation normal and abnormal image and its LL part at fourth level  $a_4$  is given in Fig.2.

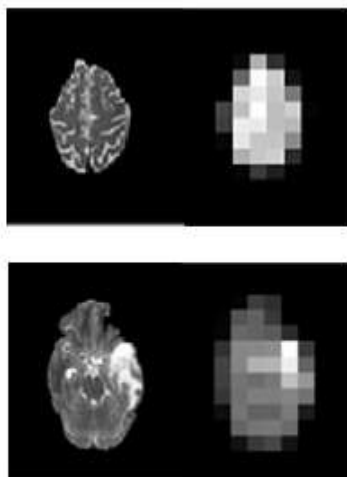


Figure 2. DWT applied on normal and abnormal images. Row 1 contains normal image and its approximation section  $a_4$ . Row 2 contains normal image and its approximation section  $a_4$

The first row shows the normal brain image which has evenly distributed CSF throughout the image. But higher intensity is in the middle of wavelet transformed image  $a_4$ . In the next image which shows in row 2 contains tumour in frontal lobe. The location of tumour shows higher intensity than the ventricles. For locality detection, each pixel in  $a_4$

is indexed as Fig.3. The wavelet transformed normal image in Fig. 2, row 1 shows higher intensity at pixel index 64 and the abnormal image which is shown in row 2 of Fig. 2 shows higher intensity at pixel index 90. Thus indicates that the pixel indexes from 61 to 66 and 75 to 80 are considered as ventricle region. Higher intensity at these pixel indexes represents the lower choice of abnormality. But some types of tumours appear in centre part of the axial brain image. Hence, probability assignment needs to fix this feature. Divide all pixels in  $a_4$  by maximum intensity. If at least anyone pixel has intensity above 0.9, at pixel indexes from 1 to 60 and 81 to 140, the output will be 1, otherwise 0. The proposed feature yields good result. But in some situation, when tumour appears in frontal or occipital lobe exactly, this feature cannot distinguish abnormal images alone. Hence, mean, standard deviation and variance of  $a_1$  are considered as supporting features.

### C. Classification

SVM suits the most for classification troubles with small training dataset and high dimensional feature space. It also needs two preparation stages, training and testing stage. SVM trains itself by given features. For training, it uses more mathematical formulations which are called kernel functions that map the training data into kernel space. The kernel is double fold by mapping the input to adequately large feature space. This mapping generates patterns that will make classification work easier. Four types of SVM kernels are available. They are linear, quadratic, radial basis function (RBF) and polynomial. Linear kernel is best to apply on linearly separable data, quadratic kernel is less computational intensive. RBF kernel is useful in vectors which are nonlinearly mapped to a very high dimension feature space. A polynomial kernel is also allows learning non-linear proved RBF kernel function is best for all. In testing volume the tumour images will be continuous that is linear. Hence, the proposed algorithm chooses linear kernel for learning. This linear kernel function with the wavelet feature set is used to build support vectors for classification.

|    |    |    |    |    |    |    |     |     |     |
|----|----|----|----|----|----|----|-----|-----|-----|
| 1  | 15 | 29 | 43 | 57 | 71 | 85 | 99  | 113 | 127 |
| 2  | 16 | 30 | 44 | 58 | 72 | 86 | 100 | 114 | 128 |
| 3  | 17 | 31 | 45 | 59 | 73 | 87 | 101 | 115 | 129 |
| 4  | 18 | 32 | 46 | 60 | 74 | 88 | 102 | 116 | 130 |
| 5  | 19 | 33 | 47 | 61 | 75 | 89 | 103 | 117 | 131 |
| 6  | 20 | 34 | 48 | 62 | 76 | 90 | 104 | 118 | 132 |
| 7  | 21 | 35 | 49 | 63 | 77 | 91 | 105 | 119 | 133 |
| 8  | 22 | 36 | 50 | 64 | 78 | 92 | 106 | 120 | 134 |
| 9  | 23 | 37 | 51 | 65 | 79 | 93 | 107 | 121 | 135 |
| 10 | 24 | 38 | 52 | 66 | 80 | 94 | 108 | 122 | 136 |
| 11 | 25 | 39 | 53 | 67 | 81 | 95 | 109 | 123 | 137 |
| 12 | 26 | 40 | 54 | 68 | 82 | 96 | 110 | 124 | 138 |
| 13 | 27 | 41 | 55 | 69 | 83 | 97 | 111 | 125 | 139 |
| 14 | 28 | 42 | 56 | 70 | 84 | 98 | 112 | 126 | 140 |

Figure 3. Pixel index at 14 × 10

D. Abnormal Tissue Location Detection

1) Block Separation

In a4 the original image should be transformed to 14×10 blocks. Hence, the original image size was initially checked whether it can perfectly make 14X10 blocks. If it is not fit to produce even sized blocks, the size to be increased by adding zero row or column in the 4 sides of the image. Then the image was divided into 140 blocks. The pixels which are getting more than 0.9 in a4 are mapped to the 140 blocks. Then these blocks were taken for the tumour location detection as given in Fig. 4.

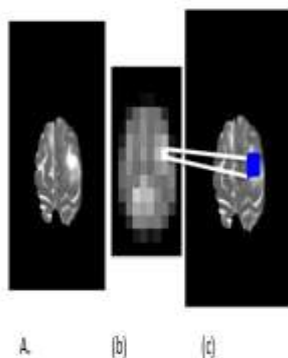


Figure 4. Tumor location detection from its feature (a) Abnormal image, (b) DWT transformed image a4 and (c) Tumor locate image

2) . Error measures

More different soft tissues are combined to made brain. In MRI they appear in different contrast due to its characteristics. Hence, a pixel block consists of normal brain tissues in size 14×10 should contain more different contrast pixels than abnormal

tumor pixels. It makes more intensity deviations between each pixel and its neighbors. Hence, MAPE is implemented to detect their inhomogeneity. The mean of pixels in a block is taken as M, the actual intensity of each pixel is taken as B. Then the error will be calculated as,

$$MAPE_b = \frac{1}{n} \sum_{i,j=1}^{m,n} \frac{|M - B_{i,j}|}{M} \times 100$$

(1)

Tumor location is detected by

$$TL = \min \{MAPE_b\}$$

(2)

where n represents the number of pixels in a block and b represents block. Among all blocks, the minimum MAPE is selected as tumor location. It yields more accurate results. Finally, the newly added rows and columns are removed from the original abnormal image.

III. RESULTS AND DISCUSSION

For the experiments, skull striped T2-w images were collected from BRATS website which contains images captured from various machines images. 20 high grade 3D real volumes were selected for the experiments. The 3D images were converted into 2D magnitude images with the help of 3D images 43.0 and MRICRO software. Then the above algorithm is coded using Matlab 7.8. Avinash Uppuluri’s Matlab tool box is used for GLCM based feature extraction.

For the performance evaluation the results of proposed work were compared with the following methods.

Avinash method – The classifier result based on GLCM features produced by Avinash Uppuluri’s Matlab tool box. The features are Angular second moment, contrast, homogeneity, entropy, correlation, variance, average, sum entropy, difference entropy, inertia, cluster shade and cluster prominence [16].

Hybrid method – The classifier results based on both proposed wavelet features and Avinash’s GLCM features.

Kalaiselvi’s method – The tumour segmentation based on brain symmetric property [3].

Kalaiselvi’s Wpack method – This method applies wavelet packet transformation in images. Then find singular points using modulus maxima equation. The singular points are traced and then displayed as tumour tissues (7).

**TABLE I.** RESULT OF CLASSIFICATION WITH GLCM, PROPOSED AND BOTH

| Volume ID<br>(1) | FA%           |                |                 | MA%           |                |                 | Volume ID<br>(1) | FA%           |                |                  | MA%            |                 |                  |
|------------------|---------------|----------------|-----------------|---------------|----------------|-----------------|------------------|---------------|----------------|------------------|----------------|-----------------|------------------|
|                  | Hybrid<br>(2) | Avinash<br>(3) | Proposed<br>(4) | Hybrid<br>(5) | Avinash<br>(6) | Proposed<br>(7) |                  | Hybrid<br>(8) | Avinash<br>(9) | Proposed<br>(10) | Hybrid<br>(11) | Avinash<br>(12) | Proposed<br>(13) |
| HG1              | 8.53          | 2.33           | 0               | 12.4          | 13.95          | 14.7            | HG11             | 16.95         | 12.71          | 16.1             | 27.12          | 17.8            | 15.3             |
| HG2              | 7.09          | 7.8            | 2.84            | 0             | 2.13           | 2.13            | HG12             | 37.04         | 21.48          | 25.19            | 16.3           | 16.3            | 17.8             |
| HG3              | 12.86         | 2.86           | 0               | 13.57         | 18.57          | 15              | HG13             | 42.06         | 37.3           | 31.75            | 1.59           | 7.14            | 1.59             |
| HG4              | 12            | 8              | 7.2             | 20.8          | 16             | 13.6            | HG14             | 38.69         | 34.31          | 29.2             | 1.46           | 6.57            | 1.46             |
| HG5              | 17.27         | 4.32           | 8.63            | 4.32          | 8.63           | 8.63            | HG15             | 20.55         | 6.85           | 14.38            | 14.38          | 11.64           | 10.3             |
| HG6              | 2.08          | 1.39           | 0               | 51.39         | 32.64          | 30.6            | HG22             | 5.76          | 10.07          | 0                | 41.01          | 26.62           | 24.5             |
| HG7              | 24.41         | 22.83          | 20.47           | 12.6          | 15.75          | 15              | HG24             | 11.36         | 20.45          | 12.88            | 15.15          | 6.82            | 9.09             |
| HG8              | 3.85          | 2.31           | 0               | 0.77          | 6.15           | 3.85            | HG25             | 7.3           | 13.87          | 9.49             | 6.57           | 0               | 0.73             |
| HG9              | 4             | 4.8            | 0               | 12.8          | 9.6            | 9.6             | HG26             | 6.45          | 5.65           | 0                | 14.52          | 7.26            | 5.65             |
| HG10             | 26.21         | 20.69          | 22.76           | 0             | 0              | 0               | HG27             | 11.76         | 11.76          | 9.56             | 2.94           | 2.21            | 4.41             |
| Average          |               |                |                 |               |                |                 |                  | 15.81         | 12.59          | 10.52            | 13.48          | 11.29           | 10.2             |

The strength and limitations of the proposed novel features are analyzed using SVM classifier. For the supporting feature selection work, some normal and abnormal images were selected. Then DWT employed on those images up to one scale. From its results, mean, variance and standard deviation were selected from approximation section a1 as supporting features. These features are highly distinguishing the normal and abnormal images.

Among the 20 tumour volumes 32 normal and 28 abnormal images were selected from the volumes HG1, HG2, HG12, HG13, HG25, HG26 and HG27. In this figure, Fig. 4(a) to Fig. 4(c) are abnormal images and Fig. 4(d) to Fig. 4(f) are normal images. These are very complex to analyze for non medical personals. Features were extracted from the training images and then given as input to SVM to train it. Then this trained SVM was employed in all volumes. In the same manner, experiment has done with the twelve GLCM features. For further analysis, hybrid feature set was employed to perform training and testing of classification in all volumes. In all experiments, same training images were used. For the quantitative evaluation, false alarm (FA) and missed alarm (MA) have been used. FA indicates that the input scan without tumour is marked as abnormal during analysis. MA indicates inverse of FA [3]. The results are illustrated in Table 1. In this table, column 1 represents the volume ID, column 2, 3 and column

4 contain the FA% of hybrid, Avinash’s GLCM and proposed wavelet feature sets respectively.

Column 5, 6 and 7 contain the MA% of hybrid, Avinash’s GLCM and proposed wavelet feature sets respectively. From these results, wavelet features helps to avoid false results in the volumes HG1, HG2, HG6, HG8, HG9, HG22 and HG26 and gives very low missed alarm for the volumes HG8, HG10, HG13, HG14 and HG25. Except HG2 and Hg13 remaining volumes are unknown testing volumes. In these volumes proposed feature set yields good results. The overall performance is measured by mean of all results. It gives that the proposed feature sets

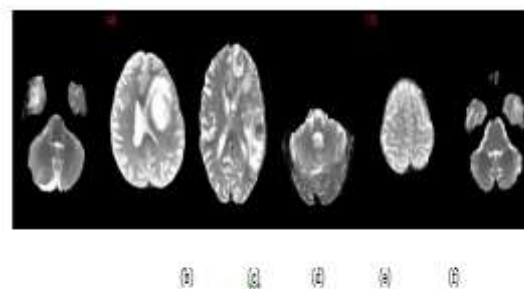


Figure 5. Training image samples. (a) to (c) are abnormal images and (d) to (e) are normal images

TABLE II. RESULT OF CLASSIFICATION WITH GLCM, PROPOSED AND BOTH ON CLINICAL DATA SET

| Volume ID<br>(1) | FA%                     |                     |                        |                       | MA%                     |                     |                        |                       |
|------------------|-------------------------|---------------------|------------------------|-----------------------|-------------------------|---------------------|------------------------|-----------------------|
|                  | Kalaiselvi's method (2) | Hybrid features (3) | Avinash's features (4) | Proposed features (5) | Kalaiselvi's method (6) | Hybrid features (7) | Avinash's features (8) | Proposed features (9) |
| v1               | 0                       | 0                   | 0                      | 0                     | 0                       | 0                   | 0                      | 0                     |
| v2               | 0                       | 0                   | 0                      | 0                     | 0                       | 0                   | 0                      | 0                     |
| v3               | 0                       | 0                   | 0                      | 0                     | 0                       | 9                   | 25                     | 9                     |
| v4               | 13                      | 6                   | 3                      | 0                     | 0                       | 0                   | 0                      | 0                     |
| v5               | 0                       | 25                  | 25                     | 16                    | 13                      | 0                   | 0                      | 4                     |
| v6               | 13                      | 0                   | 4                      | 0                     | 7                       | 16                  | 16                     | 16                    |
| v7               | 0                       | 26                  | 17                     | 27                    | 7                       | 0                   | 0                      | 0                     |
| v8               | 0                       | 4                   | 4                      | 0                     | 25                      | 8                   | 8                      | 12                    |
| Average          | 3.25                    | 7.625               | 6.625                  | 5.375                 | 6.5                     | 4.125               | 6.125                  | 5.125                 |

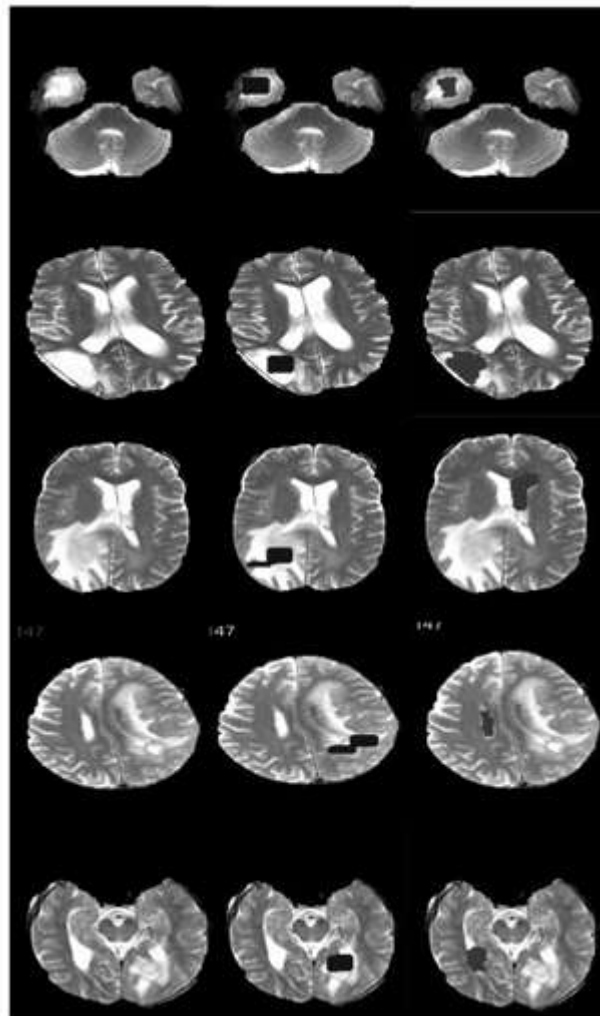


Figure 6. Tumor location detection. First column shows the tumor affected images, column2 shows the result of proposed method and column3 shows the result of Wpack

the experiment is done over with clinical images. Eight clinical volumes were selected for the experiment. Previous training images cannot yield

perfect results. Hence, totally 14 normal and abnormal images were selected as training set from v1, v2, v3 and v4. In these volumes, v1 and v2 had

obtained from normal patients. It is the real challenge for classification. The existing work [3] had detected normal volume as normal. Hence, the proposed wavelet features are employed on SVM to classify the clinical image volumes. The results of this experiment are given in Table 2. The FA and MA of existing Kalaiselvi's method is given in Table 2 at column 2 and column 6 respectively. The FA and MA of hybrid, Avinash's GLCM and proposed are given in columns 3, 4, 5, 7, 8 and 9. The proposed feature set correctly identified the normal volumes v1 and v2 as normal. Additionally, it yields 0% FA for all volumes except v5 and v7. While comparing against the existing work, the Kalsiselvi's method gives lower FA and the hybrid feature set yields lower MA. But while comparing to supervised algorithms, proposed method yields lower FA. It ensures that the performance of the proposed method. The results ensure that the selection of training volume is essential for the best performance. If some more images from v7 were selected as training volume, the proposed method can yield good results. The less number of features is another advantage of the proposed feature set. It is very easy to use and consumes less time. From this experimental study, the proposed feature set can play a vital role in abnormal image selection.

Twenty abnormal slices were taken to examine the exact tumour location detection method. In these sample abnormal slices, some sample images contain same quantity and intensity of tumour tissues and CSF. Some sample images contain the tumour nearby ventricles. For the comparison, the results of the proposed method and the results of existing Wpack method is given in Fig. 6. In this figure, the images taken for analysis are given in column1, column 2 contains the results of the proposed method. The detected regions are highlighted by dark shade. Third column shows the results of the existing Wpack method. For the first two row image, the proposed and the existing methods fit the tumour locations exactly. In the images from row 3 to row 5 tumour pixels are differentiable by its intensities. But CSF are in high intensity and not differentiable. The existing method Wpack only locate tumour according to singularity property. Hence, it detects CSF regions instead of tumour regions. The proposed method only concentrates on the summation of its neighbour and MAPE error measure. Hence, it can locate tumour correctly. Among twenty images the proposed method correctly locate tumour for seventeen images. The Wpack locate tumour for ten images. It ensures that the proposed method can locate tumour in abnormal slices well.

#### IV. CONCLUSIONS

This paper proposed a novel wavelet based feature for tumor classification. Along with this feature, mean, variance and standard deviation are also chosen for the experiment to classify abnormal images. Then abnormal tumour location detected using MAPE measure in abnormal slices. The experiments were done over the BRATS data set and clinical data sets. For the feature analysis, the proposed features were employed in SVM classifier. It proved that the proposed feature set yields good results compared to the existing GLCM feature set. The tumour location detection process was compared against an existing method Wpack. The proposed method outperforms the Wpack.

#### REFERENCES

- [1]. Kalaiselvi T. Brain portion extraction and brain abnormality detection from magnetic resonance imaging of human head scans[M]. Pallavi publications S. India pvt. Ltd., 2011
- [2]. Bauer S, Wiest R, Nolte L-P, Reyes M. A survey of MRI based medical image analysis for brain tumor studies[J]. Physics in Medicine and Biology. 2013, 58: R97-R129.
- [3]. Somasundaram K, Kalaiselvi T. Fully Automatic method to Identify Abnormal MRI Head Scans using Fuzzy Segmentation and Fuzzy Symmetric Measure[J], ICGST-GVIP Journal. 2010, 10(3):1-9.
- [4]. Shah S, Chauhan N.C. Classification of brain MRI images using computational intelligencetechniques[J], International journal of computer applications. 2015, 124(14):27-35.
- [5]. Kalaiselvi T, Kumarashankar T, Sriramakrishnan P. Nagaraja P. Novel statistical feature for Brain Abnormality Detection process in image mines of MRI Head volumes[C], National conference on 2015 recent advance in computer science and Applications, 119-123.
- [6]. Narmatha D, cruz sudheesh K V. Brain Abnormality Detection in MRI image based an Estimation of statistical Texture measures[J], International Journal of Innovative science, Engineering & technology. 2015, 4:633-638.
- [7]. Kalaiselvi T, Karthigai Selvi S. An automatic method to locate tumor from MRI brain images using wavelet packet based feature set[C], Rajendran Prasath and Kathivalavakumar 2013 (Eds.), 224-233.
- [9]. Selvaraj H, Thamarai selvi S, Selvathi D, Gewali L. Brain MRI slices classification using least squares support vector machine[J], International journal of intelligent computing in medical sciences and image processing. 2007, 1: 21-33.
- [10]. Jeyachandran, Dhanasekaran R. Brain tumor Detection and classification of MR images using Texture feature and fuzzy SVM classifier[J], Research Journal of Applied sciences, Engineering and Technology. 2013, 12:2263-2269.
- [11]. Singh B, Singh J. Classification of brain MRI in wavelet domain[J], International journal of engineering in computer science. 2011, 1:879-885.

- [12]. Chandra S Bhat, R Singh H, Chauhan D. Selection of brain tumors from MRI using Gaussian RBF kernel based support vector machine[J], International journal of advancements in computer technology. 2009, 1:46-51.
- [13]. Ahmad M, Hassa M, Imran Shafi, Osman A. Classification of tumors in human brain MRI using wavelet and support vector machine[J], International organization of scientific research. 2012, 8:25-31.
- [14]. Lashkari A E, A neural network based method for brain abnormality detection in MR images using Gabor wavelets[J], International journal of computer application. 2010, 4:841- 847.
- [15]. Amien M, Ibrahim W A A. An Intelligent model for Automatic Brain Tumor Diagnosis based on IMRI Images[J], International Journal of computer Applications. 2013, 23:21-24.
- [16]. Somasundaram K, Kalaiselvi T. Fully automatic brain extraction algorithm for T2-weighted magnetic resonance images[J]. Computers in biology and medicine, 2010, 40:811-822.
- [17]. [http://www.mathworks.com/matlabcentral/newsreader/view\\_thread/239608](http://www.mathworks.com/matlabcentral/newsreader/view_thread/239608)

S. Karthigai Selvi " DWT Based Method to Locate Tumor from T2-W Axial Head Scans" International Journal of Engineering Research and Applications (IJERA), Vol. 09. No.03. 2019. pp. 63-70